

Tau polarization in SUSY cascade decays at LHC^{*}

Kentarou Mawatari^a

School of Physics, Korea Institute for Advanced Study (KIAS), Seoul 130-722, South Korea

Abstract. We explore how the polarization of the tau leptons in the cascade decay $\tilde{q} \rightarrow q\tilde{\chi}_2^0 \rightarrow q\tau\tilde{\tau} \rightarrow q\tau\tau\tilde{\chi}_1^0$ can be exploited to study mixing properties of neutralinos and staus. We present details of the analysis including experimental effects such as transverse momentum cuts for the $\tau \rightarrow \pi\nu$ decay mode, and show that the di-pion invariant mass distribution provides valuable information on their properties.

PACS. 14.80.Ly Supersymmetric partners of known particles – 13.85.Hd Inelastic scattering: many-particles final states

1 Introduction

At LHC squarks and gluinos will be copiously produced, and cascade down, generally in several steps, to the lightest supersymmetric particle (LSP), which is stable in R -parity conserving scenarios. Though the LSPs escape detection, the kinematic edge measurements of the visible final state in various combinations of quark jets and leptons can serve to study the precision with which the masses of supersymmetric particles can be measured at LHC, for a summary see Ref. [1]. In addition, invariant mass distributions have been studied to determine the slepton mixing [2] and the spin of the particles involved [3, 4, 5, 6], shedding light on the nature of the new particles observed in the cascade and on the underlying physics scenario.

So far, cascades have primarily been studied involving first and second generation leptons/sleptons. Recently we explored how the polarization of τ leptons can be exploited to study R/L chirality and mixing effects in both the neutralino and the stau sectors [7]. In this report, we demonstrate whether measuring the correlation of the τ polarizations provides an excellent instrument to analyze these effects,¹ using a event generator.

2 Tau polarization analyzer

As polarization analyzer we use single pion decays of the τ 's. At high energies the mass of the τ leptons can be neglected and the fragmentation functions are

linear in the fraction z of the energy transferred from the polarized τ 's to the π 's [9]:

$$(\tau_R)^\pm \rightarrow \bar{\nu}_\tau^{(-)} \pi^\pm : \quad F_R = 2z, \quad (1a)$$

$$(\tau_L)^\pm \rightarrow \bar{\nu}_\tau^{(-)} \pi^\pm : \quad F_L = 2(1-z). \quad (1b)$$

In the relativistic limit, helicity and chirality are of equal and opposite sign for τ^- leptons and τ^+ anti-leptons, respectively. For notational convenience we characterize the τ states by chirality.

This report should serve only as an exploratory theoretical study. Experimental simulations will include other τ decay final states in addition to π 's, *e.g.* ρ 's and a_1 's. The ρ -meson mode is expected to contribute to the τ -spin correlation measurement even if the π^\pm and π^0 energies are not measured separately. In this case the τ polarization analysis power of the ρ channel is $\kappa_\rho = (m_\tau^2 - 2m_\rho^2)/(m_\tau^2 + 2m_\rho^2) \sim 1/2$ in contrast to $\kappa_\pi = 1$, but its larger branching fraction of $B_\rho \approx 0.25$, *vs.* $B_\pi \approx 0.11$, more than compensates for the reduced analysis power. Moreover, in actual experiments it should be possible to measure the π^\pm energy and the γ energies of the π^0 's, all emitted along the parent τ -momentum direction at high energies. Significant improvement of the τ analysis power is therefore expected from the ρ and a_1 modes by determining the momentum fraction of π^\pm in the collinear limit of their decays [9]. For each mode, cuts and efficiencies for τ identification must be included to arrive finally at realistic error estimates. The large size of the polarization effects predicted on the theoretical basis, and exemplified quantitatively by the pion channel, should guarantee their survival in realistic experimental environments, and we expect that they can be exploited experimentally in practice.

^{*} presented at the 15th International Conference on Supersymmetry and the Unification of Fundamental Interactions (SUSY07), July 26 - August 1, 2007, Karlsruhe, Germany.

^a Email: kentarou@kias.re.kr

¹ For a discussion of polarization effects in single τ decays see Ref. [8].

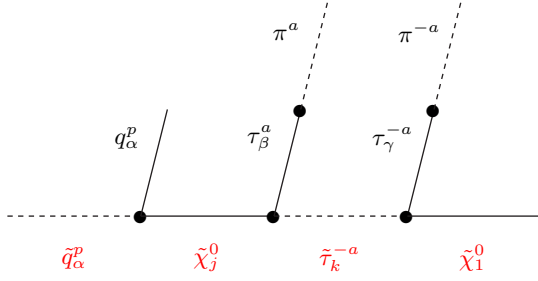


Fig. 1. The general structure of the quantum numbers of the particles involved in the squark cascade (2).

3 Squark cascade decay

We consider the squark cascade decay involving third generation leptons/sleptons

$$\tilde{q}_L \rightarrow q\tilde{\chi}_2^0 \rightarrow q\tau^\pm\tilde{\tau}^\mp \rightarrow q\tau^\pm\tau^\mp\tilde{\chi}_1^0. \quad (2)$$

At the SPS1a point [10], $\tilde{\chi}_2^0$ and $\tilde{\chi}_1^0$ are wino- and bino-like, respectively. Therefore left-handed squarks decay to $\tilde{\chi}_2^0$ with a branching ratio $\sim 30\%$, while right-handed squarks directly decay to the LSP $\tilde{\chi}_1^0$.

The distribution of the visible final state particles in the squark cascade can be cast, for massless quark and no squark mixing, in the general form [2]:

$$\begin{aligned} & \frac{1}{\Gamma_{\tilde{q}_\alpha}} \frac{d\Gamma_{\alpha\beta\gamma}^{pa;jk}}{d\cos\theta_{\tau_n} d\cos\theta_{\tau_f} d\phi_{\tau_f}} \\ &= \frac{1}{8\pi} B(\tilde{q}_\alpha \rightarrow q_\alpha \tilde{\chi}_j^0) B(\tilde{\chi}_j^0 \rightarrow \tau_\beta \tilde{\tau}_k) B(\tilde{\tau}_k \rightarrow \tau_\gamma \tilde{\chi}_1^0) \\ & \quad \times [1 + (pa)(\alpha\beta) \cos\theta_{\tau_n}] \end{aligned} \quad (3)$$

with $p = +, \alpha = -, j = 2$ and $k = 1$ for the squark chain of Eq. (2). The structure of the quantum numbers in the cascade is depicted in Fig. 1 while the configuration of the particles in the $\tilde{q}/\tilde{\chi}_2^0/\tilde{\tau}_1$ rest frames is shown in Fig. 2. For clarity the definitions are summarized in the following table:

$p = \pm :$	particle/anti-particle,
$a = \pm :$	τ and π charge,
$j = 2, 3, 4 :$	neutralino mass index,
$k = 1, 2 :$	$\tilde{\tau}$ mass index,
$\alpha = \pm :$	\tilde{q} and q R/L chirality,
$\beta = \pm :$	near τ_n R/L chirality,
$\gamma = \pm :$	far τ_f R/L chirality.

Near (n) and far (f) indices denote τ and π particles emitted in $\tilde{\chi}_j^0$ and $\tilde{\tau}_k$ decays, respectively.

The $q_\alpha \tilde{q}_\alpha \tilde{\chi}_j^0$ and the $\tau_\beta \tilde{\tau}_k \tilde{\chi}_j^0$ vertices are given by the proper current couplings and the neutralino and stau mixing matrix elements,

$$\langle \tilde{\chi}_j^0 | \tilde{q}_\alpha | q_\alpha \rangle = ig A_{\alpha\alpha j}^q, \quad (4)$$

$$\langle \tilde{\chi}_j^0 | \tilde{\tau}_k | \tau_\beta \rangle = ig A_{\beta k j}^\tau, \quad [\gamma \text{ correspondingly}] \quad (5)$$

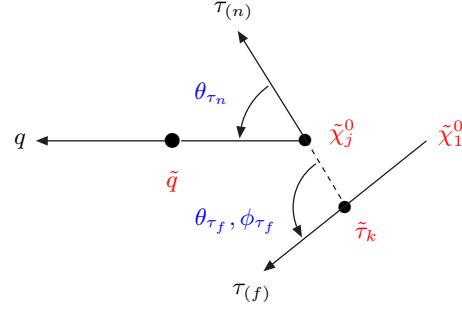


Fig. 2. The angular configuration of the particles in the $\tilde{q}/\tilde{\chi}_j^0/\tilde{\tau}_k$ rest frames.

with the explicit form of the couplings $A_{\alpha\alpha j}^q$

$$A_{LLj}^q = -\sqrt{2}[T_3^q N_{j2}^* + (e_q - T_3^q) N_{j1}^* t_W], \quad (6a)$$

$$A_{RRj}^q = +\sqrt{2}e_q N_{j1} t_W, \quad (6b)$$

and $A_{\beta k j}^\tau$

$$A_{Lkj}^\tau = -h_\tau N_{j3}^* U_{\tilde{\tau}_{k2}} + \frac{1}{\sqrt{2}}(N_{j2}^* + N_{j1}^* t_W) U_{\tilde{\tau}_{k1}}, \quad (7a)$$

$$A_{Rkj}^\tau = -h_\tau N_{j3} U_{\tilde{\tau}_{k1}} - \sqrt{2} N_{j1} t_W U_{\tilde{\tau}_{k2}}, \quad (7b)$$

in terms of the 4×4 neutralino mixing matrix N in the standard gaugino/higgsino basis and the 2×2 stau mixing matrix $U_{\tilde{\tau}}$ in the L/R basis. Here, $T_3^q = \pm 1/2$ and $e_q = 2/3, -1/3$ are the $SU(2)$ doublet quark isospin and electric charge, $t_W = \tan\theta_W$ and $h_\tau = m_\tau/\sqrt{2}m_W \cos\beta$. The distribution (3) depends only on the “near τ ” angle θ_{τ_n} ; this is a consequence of the scalar character of the intermediate stau state that erases all angular correlations.

The angles in the cascade Fig. 2 are related to the invariant masses [1,2,4],

$$m_{\tau\tau}^2 = (m_{\tau\tau}^{\max})^2 \cdot \frac{1}{2} (1 - \cos\theta_{\tau_f}), \quad (8a)$$

$$m_{q\tau_n}^2 = (m_{q\tau_n}^{\max})^2 \cdot \frac{1}{2} (1 - \cos\theta_{\tau_n}), \quad (8b)$$

$$\begin{aligned} m_{q\tau_f}^2 = (m_{q\tau_f}^{\max})^2 \cdot & \left[\frac{1}{4} (1 + c_n)(1 - c_f) - \frac{r_{jk}}{2} s_n s_f \cos\phi_{\tau_f} \right. \\ & \left. + \frac{r_{jk}^2}{4} (1 - c_n)(1 + c_f) \right], \end{aligned} \quad (8c)$$

where the maximum values of the invariant masses

$$(m_{\tau\tau}^{\max})^2 = m_{\tilde{\chi}_j^0}^2 (1 - m_{\tilde{\tau}_k}^2/m_{\tilde{\chi}_j^0}^2) (1 - m_{\tilde{\chi}_1^0}^2/m_{\tilde{\tau}_k}^2), \quad (9a)$$

$$(m_{q\tau_n}^{\max})^2 = m_{q_\alpha}^2 (1 - m_{\tilde{\chi}_j^0}^2/m_{q_\alpha}^2) (1 - m_{\tilde{\tau}_k}^2/m_{\tilde{\chi}_j^0}^2), \quad (9b)$$

$$(m_{q\tau_f}^{\max})^2 = m_{q_\alpha}^2 (1 - m_{\tilde{\chi}_j^0}^2/m_{q_\alpha}^2) (1 - m_{\tilde{\chi}_1^0}^2/m_{\tilde{\tau}_k}^2), \quad (9c)$$

$r_{jk} = m_{\tilde{\tau}_k}/m_{\tilde{\chi}_j^0}$, and abbreviations $c_n = \cos\theta_{\tau_n}$, $c_f = \cos\theta_{\tau_f}$ etc. are introduced. Note that the rescaled invariant masses, $\tilde{m}^2 \equiv m^2/(m^{\max})^2$, are used for analysis in our original paper [7].

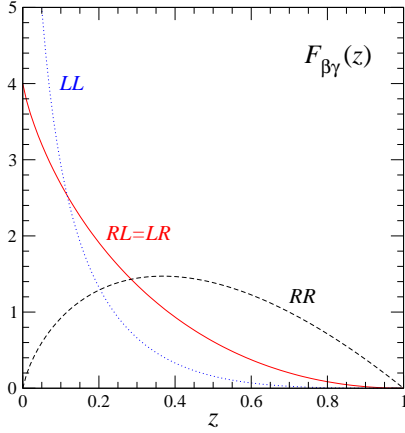


Fig. 3. Double fragmentation functions $F_{\beta\gamma}(z)$.

4 Pion invariant mass distribution

Pion invariant mass distributions, summed over near and far particles, are predicted by folding the original single τ and double $\tau\tau$ distributions, $d\Gamma_\beta/dm_{q\tau}^2$ and $d\Gamma_{\beta\gamma}/dm_{\tau\tau}^2$, with the single and double fragmentation functions F_β and $F_{\beta\gamma}$, where the indices β, γ denote the chirality indices R/L of the τ leptons. Based on standard techniques, the following relations can be derived for $[q\pi]$ and $[\pi\pi]$ distributions:

$$\frac{d\Gamma}{dm_{q\pi}^2} = \int_{m_{q\pi}^2}^1 \frac{dm_{q\tau}^2}{m_{q\tau}^2} \frac{d\Gamma_\beta}{dm_{q\tau}^2} F_\beta\left(\frac{m_{q\pi}^2}{m_{q\tau}^2}\right), \quad (10)$$

$$\frac{d\Gamma}{dm_{\pi\pi}^2} = \int_{m_{\pi\pi}^2}^1 \frac{dm_{\tau\tau}^2}{m_{\tau\tau}^2} \frac{d\Gamma_{\beta\gamma}}{dm_{\tau\tau}^2} F_{\beta\gamma}\left(\frac{m_{\pi\pi}^2}{m_{\tau\tau}^2}\right). \quad (11)$$

The single and double distributions, $d\Gamma_\beta/dm_{q\tau}^2$ and $d\Gamma_{\beta\gamma}/dm_{\tau\tau}^2$, can be derived from Eq. (3) by integration. The single $\tau_\beta \rightarrow \pi$ fragmentation function, cf. Eqs. (1a) and (1b) with $z = m_{q\pi}^2/m_{q\tau}^2$, can be summarized as

$$F_\beta(z) = 1 + \beta(2z - 1), \quad (12)$$

while the double $\tau_\beta\tau_\gamma \rightarrow \pi\pi$ fragmentation functions, with $z = m_{\pi\pi}^2/m_{\tau\tau}^2$, are given by

$$F_{RR}(z) = 4z \log \frac{1}{z}, \quad (13a)$$

$$F_{RL}(z) = F_{LR}(z) = 4\left[1 - z - z \log \frac{1}{z}\right], \quad (13b)$$

$$F_{LL}(z) = 4\left[(1+z) \log \frac{1}{z} + 2z - 2\right]. \quad (13c)$$

The shape of the distributions $F_{\beta\gamma}(z)$ ($\beta, \gamma = R, L$) is presented in Fig. 3. All distributions, normalized to unity, are finite except F_{LL} which is logarithmically divergent for $z \rightarrow 0$.

The analysis of $\pi\pi$ invariant mass, *etc.*, for polarization measurements in cascades does not require the experimental reconstruction of τ -jet energies, in contrast to the fraction R of charged π over τ energy, see Ref. [11].

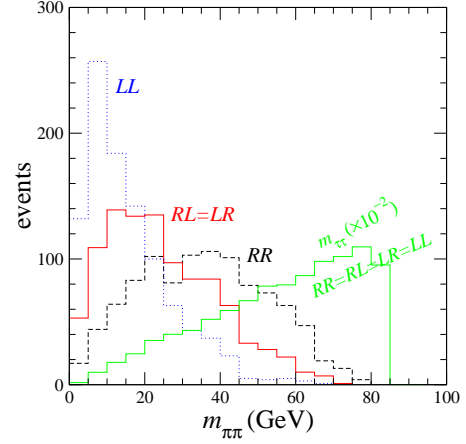


Fig. 4. Di- π invariant mass distributions in the $\tilde{\chi}_2^0$ decays of the cascade (2). The indices denote the chiralities of the near and far τ leptons. The di- τ invariant mass distribution is also shown by a thin line.

5 Simulations

At the SPS1a point [10], the production cross section of the squarks (\tilde{u}_L and \tilde{d}_L) is 33 pb at LHC [1], and the branching fractions of the cascade (2) are $B(\tilde{q}_L \rightarrow q\tilde{\chi}_2^0) \sim 30\%$, $B(\tilde{\chi}_2^0 \rightarrow \tau\tilde{\tau}_1) = 88\%$, and $B(\tilde{\tau}_1 \rightarrow \tau\tilde{\chi}_1^0) = 100\%$. Hence, roughly 10^5 events for the cascade would be expected with $L = 10 \text{ fb}^{-1}$. In this report, taking into account the branching fraction $B(\tau \rightarrow \pi\nu)$, we estimate the di- π invariant mass distribution with 10^3 events. The events are generated by MadGraph/MadEvent [12] with the DECAY package for τ decays, and studied using MadAnalysis.

The great potential of polarization measurements for determining mixing phenomena is demonstrated in Fig. 4, displaying the di- π invariant mass distributions in the $\tilde{\chi}_2^0$ decays of the cascade (2) [13, 7]. The di- τ distribution is also shown. The maximum value of the di- τ invariant mass in Eq. (9a) is 84 GeV for the sparticle masses at SPS1a: $m_{\tilde{q}} \sim 560 \text{ GeV}$, $m_{\tilde{\chi}_2^0} = 181 \text{ GeV}$, $m_{\tilde{\tau}} = 134 \text{ GeV}$, and $m_{\tilde{\chi}_1^0} = 97 \text{ GeV}$. While the lepton-lepton invariant mass does not depend on the chirality indices of the near and far τ leptons, the shape of the π distribution depends strongly on the indices, as expected.

Fig. 5 shows the di- π invariant mass distribution in the \tilde{q} decays of the cascade (2) at SPS1a. The hypothetical RR - and LL -type distributions are also shown by dashed and dotted lines, respectively, for comparison. The solid line for SPS1a clearly indicates that the near/far τ couplings are RL - or LR -dominated (cf. Fig. 4). This can be traced back to the fact that $\tilde{\chi}_2^0$ is nearly \tilde{W} -like and $\tilde{\tau}_1$ is nearly $\tilde{\tau}_R$ -like at SPS1a, which is reflected in the $\tau_\beta\tilde{\tau}_k\tilde{\chi}_j^0$ coupling, $A_{\beta kj}^\tau$, in Eqs. (7a) and (7b). The magnitude of the couplings are

$$\begin{aligned} |A_{L12}^\tau| &= 0.240, & |A_{R12}^\tau| &= 0.0626, \\ |A_{L11}^\tau| &= 0.0763, & |A_{R11}^\tau| &= 0.745, \end{aligned} \quad (14)$$

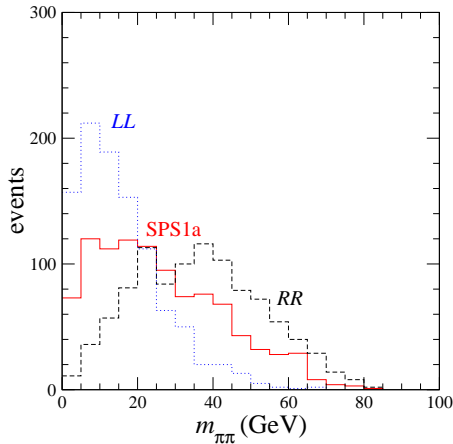


Fig. 5. Di- π invariant mass distribution in the \tilde{q} decays of the cascade (2) at SPS1a. The dashed and dotted lines indicate the hypothetical RR - and LL -type distributions, respectively, for comparison.

and the polarization of the near (far) τ leptons, $\tau_{n(f)}$, is given in the $m_\tau \ll m_{\tilde{\tau}_1}$ limit as

$$P_{\tau_{n(f)}} = \frac{|A_{R12(1)}^\tau|^2 - |A_{L12(1)}^\tau|^2}{|A_{R12(1)}^\tau|^2 + |A_{L12(1)}^\tau|^2}. \quad (15)$$

Therefore, the polarization of the near τ is almost left-handed ($P_{\tau_n} = -0.873$), while the far τ has the right-handed polarization ($P_{\tau_f} = +0.979$). This leads the LR -dominated distribution in the di- π invariant mass.

Finally we briefly study the effects of the experimental cut on the π transverse momenta. Experimental analyses of τ particles are a difficult task at LHC. Isolation criteria of hadron and lepton tracks must be met which reduce the efficiencies strongly for small transverse momenta. Stringent transverse momentum cuts increase the efficiencies but reduce the primary event number and erase the difference between R and L distributions. On the other hand, fairly small transverse momentum cuts reduce the efficiencies but do not reduce the primary event number and the R/L sensitivity of the distributions. Optimization procedures in this context are far beyond the scope of this report. Experimental details for di- τ final states for the cascades at LHC may be studied in the recent notes [14].

In Fig. 6 it is shown how a cut of 10 GeV on the π transverse momenta modifies the distributions of the di- π invariant mass in Fig. 5. 75%, 55%, and 32% of the events for RR -type, SPS1a, and LL -type, respectively, survive the selection. The RR -type distribution is mildly affected while the LL -type is shifted more strongly. The different size of the shifts can be traced back to the different shapes of the R and L fragmentation functions. Since L fragmentation is soft, more events with low transverse momentum are removed by the cut and the shift is correspondingly larger than for hard R fragmentation. Apparently, the peak positions of the distributions are still different, and the transverse momentum cut does not erase the distinctive difference between them.

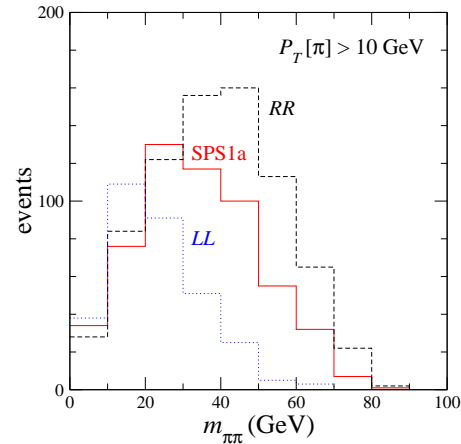


Fig. 6. The same as Fig. 5 with a kinematic cut of 10 GeV on the π transverse momenta.

6 summary

The analysis of τ polarization in cascade decays provides valuable information on chirality-type and mixing of supersymmetric particles. The exciting effects are predicted for the invariant mass distributions in the di- π sector generated by the two polarized τ decays. Note that these effects are independent of the couplings in the \tilde{q}/q sector and also of the polarization state of $\tilde{\chi}_2^0$. See more details in Ref. [7].

Acknowledgements

The author thanks S.Y. Choi, K. Hagiwara, Y.G. Kim, and P.M. Zerwas for the collaboration.

References

1. G. Weiglein *et al.*, Phys. Rept. **426** (2006) 47.
2. T. Goto, K. Kawagoe and M. M. Nojiri, Phys. Rev. D **70** (2004) 075016 [Erratum-ibid. D **71** (2005) 059902].
3. A. J. Barr, Phys. Lett. B **596** (2004) 205.
4. J. M. Smillie and B. R. Webber, JHEP **0510** (2005) 069; C. Athanasiou, C. G. Lester, J. M. Smillie and B. R. Webber, JHEP **0608** (2006) 055.
5. A. Datta, K. Kong and K. T. Matchev, Phys. Rev. D **72** (2005) 096006 [Erratum-ibid. D **72** (2005) 119901].
6. L. T. Wang and I. Yavin, JHEP **0704** (2007) 032.
7. S. Y. Choi, K. Hagiwara, Y. G. Kim, K. Mawatari and P. M. Zerwas, Phys. Lett. B **648** (2007) 207.
8. M. M. Nojiri, Phys. Rev. D **51** (1995) 6281; M. M. Nojiri, K. Fujii and T. Tsukamoto, Phys. Rev. D **54** (1996) 6756.
9. B. K. Bullock, K. Hagiwara and A. D. Martin, Nucl. Phys. B **395** (1993) 499.
10. B. C. Allanach *et al.*, Eur. Phys. J. C **25** (2002) 113.
11. M. Guchait and D. P. Roy, Phys. Lett. B **541** (2002) 356.
12. J. Alwall *et al.*, JHEP **0709** (2007) 028; <http://madgraph.phys.ucl.ac.be/>.
13. R. N. Cahn, in *Proc. of Snowmass 96, Snowmass, Colorado, 25 Jun - 12 Jul 1996, pp SUP113*.
14. D. J. Mangeol and U. Goerlach, CMS note 2006/096.